Dynamics and Control of a Quadrotor with a Payload Suspended through an Elastic Cable

Prasanth Kotaru[1], Guofan Wu[1] and Koushil Sreenath[2]

***Abstract*— We study the problem of a quadrotor transporting a payload suspended through a cable. While prior work has modeled the cable as a massless rigid link, in this paper, we consider the cable to be elastic with both spring stiffness and damping. We derive a coordinate-free dynamical model of the system. We use singular-perturbations to show that a geometric controller developed for the case of an inelastic cable still works for the case of an elastic cable to achieve almost global exponential tracking of a desired load position to within a certain bound. We provide numerical results to validate the proposed controller for various spring and damping coefficients for the cable.**

I. Introduction

Aerial robotics has shown great promise in recent years with potential applications in areas of surveillance, transportation, and agriculture. In particular, the rise of small-sized, commercial unmanned aerial vehicles (UAV) has enabled the possibility of point-to-point aerial transportation. To achieve a reliable and efficient transportation using small UAVs, researchers have proposed various methods in design, planning, and control.

In terms of mechanical design, several methods have been proposed to attach a payload to a UAV, involving both active and passive attachments. Examples of active attachments include using actuated grippers to grip and pickup payloads [13], [10], and actuated manipulator arms to enable aerial manipulation [10]. These active mechanisms provide more degrees-of-freedom (DOFs) to the UAV, and help in active aerial manipulation. However, these advantages come at the cost of loss of agility of the small UAVs due to the added inertia to the system. Moreover, actuated gripper arms introduce dynamic coupling between the manipulator and quadrotor which needs to be accurately captured in the mathematical model and compensated by the controller.

Passive type of attachments have also been developed, wherein the payload is attached to the UAVs through a mechanical cable or tether [2], [15], [17], [6], [18]. By attaching the payload through tethers, the payload could be connected to a single or multiple UAVs without directly modifying the UAV's inertia. However, this becomes more challenging for control due to the additional degree-of-underactuation. Early work looked at the transportation of a single point-mass load with single and multiple helicopters [2], with the objective being to actively cancel any swing in the cable. Furthermore, dynamic programming (DP) based methods were employed to plan dynamically-feasible trajectories that minimized the load swing along with an adaptive controller in [15].

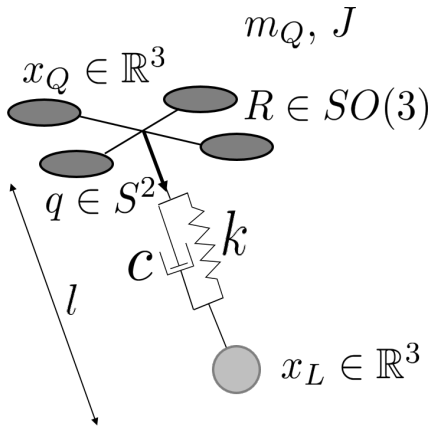

Fig. 1: Quadrotor with load through a suspended cable, with the cable modeled as a spring-damper. The configuration space of the system is given as $\mathbb{R}^3 \times SO(3) \times S^2 \times \mathbb{R}$, with 9 degrees-of-freedom and 4 actuators, resulting in 5 degrees-of-underactuation.

Instead of actively canceling out the cable's swing, resulting in slow quasi-static motion, one can explicitly study the coupling effects of the suspended payload and the quadrotor to enable rapid dynamic motions, as done in [17], [6], [18]. The idea is to model the cable as a massless rigid rod when it is taut and model the transitions between the cable going from taut to slack, and slack to taut as discrete transitions using hybrid system analysis. Based on the massless rigid rod model, prior work [17] has derived the dynamics of a single quadrotor with suspended load and developed a geometric controller to exponentially track the load's position. Moreover, the quadrotor with a suspended load is also established as a differentially-flat hybrid system, enabling fast motion planning in the flat-space. These results were used in [18] to plan dynamically-feasible trajectories that transition the cable from taut to slack and back, to avoid collision with obstacles. The problem of geometric control of multiple quadrotors with a suspended point-mass load [12] and with a rigid-body load [11], [19] has also been studied. More recently, the cable has also been modeled as a flexible chain of links with mass, and a set-point regulation control based on the linearized model has been demonstrated in [7].

While all the previous work has considered the cable to be

[1]P. Kotaru, G. Wu are with Department of Mechanical Engineering, Carnegie Mellon University, 5000 Forbes Avenue, Pittsburgh PA, 15213, email: {vkotaru,gwu}@andrew.cmu.edu.

K. Sreenath is with the Depts. of Mechanical Engineering, The Robotics Institute, and Electrical and Computer Engineering, Carnegie Mellon University, Pittsburgh, PA 15213, email: koushils@cmu.edu.

This work is supported in part by the Google Faculty Research Award and in part by NSF grants CMMI-1538869, IIS-1464337, IIS-1526515.

inelastic, we are motivated by extensive studies in robotics and space applications with cable tethers where elasticity in the tether cannot be ignored in practice, see [8], [1], [4]. This makes the massless rigid rod model not accurate enough to estimate the cable's behavior and requires the introduction of compliance and damping. In particular, the taut cable tether was modeled as linear elasticity in [8], and in [1] for surgical robot applications . In general, for most applications, a unilateral linear spring model will more accurately represent the cable dynamics.

Here, we study the problem of a quadrotor transporting a point mass payload suspended through an elastic cable. The goal is to investigate the effect of an elastic cable and compare the corresponding dynamics and control performance with prior work. The contributions of this paper with respect to prior work are,

- We consider the quadrotor with a cable-suspended payload and model the cable as a linear spring with damper. We derive the dynamics in a coordinate-free manner using Hamilton's principle of least action.
- We show that the same geometric controller developed in [16], wherein the cable was assumed to be inelastic, still works when the cable is elastic. We provide a formal stability analysis using singular perturbations.
- We present numerical results of tracking the load position for various cable stiffness properties to numerically validate the performance of our proposed controller.

The rest of the paper is structured as follows. Section II derives and presents the corresponding dynamics with comments; Section III proposes a geometric control method, where a stability analysis using singular perturbations is provided. Section IV shows the simulation results, of a quadrotor carrying a load with elastic tether, with tracking errors. Section V summarizes the works and draws the final conclusion.

II. Dynamical model of quadrotor with spring-damper suspended load

We develop a coordinate-free dynamic model for a quadrotor with a cable-suspended load, wherein the cable is modeled as a spring-damper. The dynamic model is defined using a geometric representation, with the quadrotor attitude represented by a rotation matrix $SO(3) := \{R \in \mathbb{R}^{3\times3} | R^T R = I, det(R) = +1\}$ and the load attitude represented by a two-sphere $S^2 := \{q \in \mathbb{R}^3 | q.q = 1\}$.

The configuration space for the given system is, $Q = SE(3) \times S^2 \times \mathbb{R}^1$, with 9 degrees of freedom being the quadrotor orientation, $R \in SO(3)$, quadrotor position, $x_Q \in \mathbb{R}^3$, and load attitude, $q \in S^2$, and length of the spring $l \in \mathbb{R}$. The thrust magnitude $f \in \mathbb{R}$, and the moment vector $M \in \mathbb{R}^3$, form the 4 inputs to the system. Figure 1 illustrates the system under consideration.

Remark 1. *Although the quadrotor with a (inelastic) cable-suspended load is shown to be a differentially-flat system in [17], the quadrotor with elastic-cable-suspended load is not differentially-flat. This is due to the additional degree of under-actuation caused by the presence of the spring.*

$m_Q \in \mathbb{R}$	Mass of the quadrotor
$J \in \mathbb{R}^{3\times3}$	Inertia matrix of the quadrotor with respect to the body-fixed frame
$R \in SO(3)$	Rotation matrix of the quadrotor from body-fixed frame to the inertial frame
$\Omega \in \mathbb{R}^3$	Body-frame angular velocity
$x_Q, v_Q \in \mathbb{R}^3$	Position and velocity vectors of quadrotor's center of mass in the inertial frame
$q \in S^2$	Load attitude i.e., unit vector from quadrotor's center of mass to the load position
$\omega \in \mathbb{R}^3$	Angular velocity of the suspended load
$m_L \in \mathbb{R}$	Mass of the suspended Load
$x_L, v_L \in \mathbb{R}^3$	Position and velocity vectors of load position in the inertial frame
$L \in \mathbb{R}$	Free length of the spring
$l \in \mathbb{R}$	Total length of the spring
$f \in \mathbb{R}$	Magnitude of the thrust of the quadrotor
$M \in \mathbb{R}^3$	Moment vector of the quadrotor in the body-fixed frame
$k \in \mathbb{R}$	Spring constant of the suspended spring
$c \in \mathbb{R}$	Damping coefficient in the suspended spring
$\mathbf{e}_1, \mathbf{e}_2, \mathbf{e}_3 \in \mathbb{R}^3$	Unit vectors along the x,y,z directions of the inertial frame

TABLE I: Various symbols used in this paper

The dynamic model of the system is derived using Lagrangian method, where the Lagrangian of the system $\mathcal{L} : TQ \to \mathbb{R}$, is defined as,

$$\mathcal{L} = \mathcal{T} - \mathcal{U}, \tag{1}$$

where $\mathcal{T}$ is the kinetic energy of the system and $\mathcal{U}$ is the potential energy of the system. Kinetic energy $\mathcal{T} : TQ \to \mathbb{R}$ is given as,

$$\mathcal{T} = \underbrace{\frac{1}{2} m_Q \langle v_Q, v_Q \rangle + \frac{1}{2} \langle \Omega, J\Omega \rangle}_{Quadrotor\, KE} + \underbrace{\frac{1}{2} m_L \langle v_L, v_L \rangle}_{Load\, KE}, \tag{2}$$

where m_Q is mass of the quadrotor, m_L mass of the load, J moment of inertia of the quadrotor, and v_Q & v_L are the velocities of the quadrotor's center of mass and load, with Ω being the body frame angular velocity of the quadrotor. Potential energy $\mathcal{U} : TQ \to \mathbb{R}$ is given as,

$$\mathcal{U} = \underbrace{m_Q g \mathbf{e}_3 . x_Q}_{Quadrotor\, PE} + \underbrace{m_L g \mathbf{e}_3 . x_L}_{Load\, PE} + \underbrace{\frac{1}{2} k (L - l)^2}_{Cable\, PE}, \tag{3}$$

where x_Q and x_L are the positions of quadrotor's center of mass and load in the inertial frame. k is the stiffness of the cable, with L and l being the rest length and the total length of the cable. Table I explains various symbols used in this paper.

Note that the load position is related to the quadrotor center of mass, through the cable orientation as,

$$x_L = x_Q + lq, \tag{4}$$

and, the velocities and accelerations are related as,

$$v_L = v_Q + \dot{l}q + l\dot{q}, \tag{5}$$

$$\dot{v}_L = \dot{v}_Q + \ddot{l}q + l\ddot{q} + 2\dot{l}\dot{q}. \tag{6}$$

The term $2\dot{l}\dot{q}$ is the Coriolis effect, as there is motion both along the length of the suspended spring and also perpendicular to it, i.e, the attitude of the spring.

Equations of motion are derived using, Lagrange-d'Alembert's principle of least action, which states that the variation of the action integral is equal to the negative virtual work done by the external forces and non-conservative forces. The same is represented in (7).

$$\delta \int_{t_0}^{t_1} \mathcal{L} dt + \int_{t_0}^{t_1} \Big(\langle W_1, \hat{M} \rangle + W_2.(-c\dot{l}q) + W_3.fR\mathbf{e}_3 \Big) dt = 0 \tag{7}$$

where,

$$W_1 = R^T \delta R, \quad W_2 = (\delta l)q,$$

$$W_3 = \delta x_Q = \delta x_L - (\delta l)q - l(\delta q),$$

are variational vector fields [14] corresponding to quadrotor attitude, quadrotor position and load position respectively. The damping force in the cable is represented by $-c\dot{l}$. Infinitesimal variations satisfy,

$$\delta q = \xi \times q, \quad \xi \in \mathbb{R}^3 \ \ s.t \ \ \xi.q = 0,$$

$$\delta \dot{q} = \dot{\xi} \times q + \xi \times \dot{q},$$

$$\delta R = R\hat{\eta}, \quad \delta\hat{\Omega} = \widehat{\dot{\Omega}\eta} + \hat{\dot{\eta}}, \quad \eta \in \mathbb{R}^3,$$

$$\delta x_L = \delta x_Q + (\delta l)q + l(\delta q), \quad \delta x_L \,\&\, \delta x_Q \in \mathbb{R}^3, \delta l \in \mathbb{R},$$

$$\delta v_L = \delta v_Q + (\dot{\delta l})q + (\delta l)\dot{q} + \dot{l}(\delta q) + l(\dot{\delta q}),$$

with constraints $q.\dot{q} = 0$ and $\omega.q = 0$. δq is the infinitesimal variation on S^2 and δR is the variation on $SO(3)$.

Equations of motion derived from (7) for quadrotor with load suspended through an elastic cable are as follows,

$$\dot{x}_L = v_L, \tag{8}$$

$$\begin{aligned}(m_Q + m_L)(\dot{v}_L + g\mathbf{e}_3) \\ = (m_Q\ddot{l} + (q.fR\mathbf{e}_3) - m_Q l(\dot{q}.\dot{q}))q,\end{aligned} \tag{9}$$

$$\dot{q} = \omega \times q, \tag{10}$$

$$m_Q l\dot{\omega} = -(q \times fR\mathbf{e}_3) - 2m_Q\dot{l}\omega, \tag{11}$$

$$\dot{R} = R\hat{\Omega}, \tag{12}$$

$$J\dot{\Omega} = M - (\Omega \times J\Omega), \tag{13}$$

$$\begin{aligned}\ddot{l} = l(\dot{q}.\dot{q}) + \frac{m_Q + m_L}{m_Q m_L}k(L - l) \\ - \frac{m_Q + m_L}{m_Q m_L}c\dot{l} - \frac{1}{m_Q}(q.fR\mathbf{e}_3).\end{aligned} \tag{14}$$

Detailed derivation of these equations of motion is given in Appendix-A.

Remark 2. *In the above dynamics,* (8)-(9) *represent the load position dynamics,* (10)-(11) *show the load attitude dynamics and* (12)-(13) *represent quadrotor attitude while* (14) *shows the cable dynamics*

Remark 3. *When $l \equiv L$ is of fixed length with no spring-damper, then the equations of motion* (9)*,* (11) *can be written as,*

$$(m_Q + m_L)(\dot{v}_L + g\mathbf{e}_3) = (q.fR\mathbf{e}_3 - m_Q l(\dot{q}.\dot{q}))q, \tag{15}$$

$$m_Q l\dot{\omega} = -(q \times fR\mathbf{e}_3), \tag{16}$$

and are equal to dynamics of quadrotor with an inelastic cable suspended load [16].

Remark 4. *The suspended cable is modeled as a rigid, massless rod with stiffness and damping. In particular, we have not considered the unilateral tension constraint wherein the tension magnitude can not be negative. To accurately do this, we will need to model the system as a hybrid system with tension computed as $T = (k(L - l) - c\dot{l})q$.*

With the above computation of the tension vector, we present the quadrotor and load dynamics in Newton-Euler equations for the hybrid dynamics as below,

$$\Sigma_n : \begin{cases} m_Q(\ddot{x}_Q + g\mathbf{e}_3) = f.R\mathbf{e}_3 - T, \\ m_L(\ddot{x}_L + g\mathbf{e}_3)) = T, & l \geq L \\ (x_L^+, x_Q^+, \dot{x}_Q^+, \dot{x}_L^+) = \Delta_{n\to z}(x_L^-, x_Q^-, \dot{x}_Q^-, \dot{x}_L^-), & l = L \end{cases}$$

$$\Sigma_z : \begin{cases} m_Q(\ddot{x}_Q + g\mathbf{e}_3) = f.R\mathbf{e}_3, \\ m_L(\ddot{x}_L + g\mathbf{e}_3)) = 0, & l < L \\ (x_L^+, x_Q^+, \dot{x}_Q^+, \dot{x}_L^+) = \Delta_{z\to n}(x_L^-, x_Q^-, \dot{x}_Q^-, \dot{x}_L^-), & l = L \end{cases}$$

Here, the superscripts $.^-$, $.^+$ respectively denote the values prior to transition and post transition. The transition map $\Delta_{n\to z}$ and $\Delta_{z\to n}$ represents the transition from the tension non-zero case (cable taut) to the tension zero case (cable slack) and vice-versa. While $\Delta_{n\to z}$ can be modeled as an identity map, $\Delta_{z\to n}$ can be modeled as a perfectly inelastic collision, which causes a discrete change in the velocities.

While the above dynamical model captures the unilateral tension constraint, however for the controller discussed in the following section, we do not explicitly consider the hybrid dynamics.

III. Geometric Control Design

Having presented the dynamical model for the given system, we now discuss the control for the system. Due to the presence of the spring, there is a degree of freedom along its length which makes the control of the load position through a quadrotor a difficult problem to address. Note that the quadrotor attitude dynamics are decoupled from the other dynamics as shown in (13), while the load attitude dynamics is decoupled from the load position dynamics. Thus, a controller can be designed to achieve exponential stability for the quadrotor attitude and load attitude to track a desired (time varying) reference attitude trajectory. We will next develop a controller for tracking the load position which is coupled to the load attitude, quadrotor attitude, as well as the spring dynamics.

A. Singular Perturbation Model

In order to address the load position control we consider a singular perturbed model. As most cables have large stiffness and damping coefficients, we assume the cable stiffness k to be $(\bar{k}/\varepsilon^2)$ and the damping coefficient to be $c = (\bar{c}/\varepsilon)$, where $\bar{k}$, $\bar{c} > 0$ are finite, and ε is sufficiently small. Considering a change in co-ordinates similar to [5], we define new variables such that,

$$z_1 = \frac{l - L}{\varepsilon^2}, \tag{17}$$

$$z_2 = \frac{\dot{l}}{\varepsilon}. \tag{18}$$

Substituting the values for $k = \frac{\bar{k}}{\varepsilon^2}$, $c = \frac{\bar{c}}{\varepsilon}$, $l = L + \varepsilon^2 z_1$ and $\dot{l} = \varepsilon z_2$ in the dynamics (8)-(14), we have,

$$\dot{x}_L = v_L, \tag{19}$$

$$\begin{aligned}(m_Q + m_L)(\dot{v}_L + g\mathbf{e}_3) \\ = (m_Q \ddot{l} + (q.fR\mathbf{e}_3) - m_Q(L + \varepsilon^2 z_1)(\dot{q}.\dot{q}))q,\end{aligned} \tag{20}$$

$$\dot{q} = \omega \times q, \tag{21}$$

$$m_Q(L + \varepsilon^2 z_1)\dot{\omega} = -(q \times fR\mathbf{e}_3) - 2m_Q \dot{l}\omega, \tag{22}$$

$$\dot{R} = R\hat{\Omega}, \tag{23}$$

$$J\dot{\Omega} = M - (\Omega \times J\Omega), \tag{24}$$

$$\varepsilon \dot{z}_1 = z_2, \tag{25}$$

$$\begin{aligned}\varepsilon \dot{z}_2 = (L + \varepsilon^2 z_1)(\dot{q}.\dot{q}) + \frac{m_Q + m_L}{m_Q m_L}\bar{k}(-z_1) \\ - \frac{m_Q + m_L}{m_Q m_L}\bar{c}z_2 - \frac{1}{m_Q}(q.fR\mathbf{e}_3).\end{aligned} \tag{26}$$

The above system of equations can be represented as,

$$\dot{x} = f(t, x, z, \varepsilon), \tag{27}$$

$$\varepsilon \dot{z} = g(t, x, z, \varepsilon), \tag{28}$$

where, x represents the states x_L, v_L, q, ω, R, Ω and z corresponds to the states z_1 and z_2. Such a system model is referred as a *Singular Perturbation Model*, [9, Chapter 11]. We note that, the *fast dynamics* given by (28), which represents the dynamics in (25)-(26) can be represented as,

$$\varepsilon \frac{d}{dt}\begin{bmatrix} z_1 \\ z_2 \end{bmatrix} = \begin{bmatrix} z_2 \\ -m_r \bar{k} z_1 - m_r \bar{c} z_2 + (L + \varepsilon^2 z_1)(\dot{q}.\dot{q}) + F_1 \end{bmatrix}, \tag{29}$$

where,

$$m_r := \frac{m_Q + m_L}{m_Q m_L}, \quad F_1 := -\frac{1}{m_Q}(q.fR\mathbf{e}_3).$$

In (28), time-derivative $\dot{z}$, is given by $g(t, x, z, \varepsilon)/\varepsilon$, which is very high as ε tends to zero, implying that the dynamics of z evolve at a higher rate. Setting $\varepsilon = 0$, the system reduces to,

$$\dot{x} = f(t, x, z, \varepsilon = 0), \tag{30}$$

$$0 = g(t, x, z, \varepsilon = 0), \tag{31}$$

with the second equation being an algebraic equation given by,

$$0 = g(t, x, z, 0) \equiv \begin{bmatrix} z_2 \\ -m_r \bar{k} z_1 - m_r \bar{c} z_2 + L(\dot{q}.\dot{q}) + F_1 \end{bmatrix}, \tag{32}$$

which can be solved for z as $z = h(t, x)$. Substituting this solution for z in (30), we get *the reduced model* or *the slow model* given by,

$$\dot{x} = f(t, x, h(t, x), 0). \tag{33}$$

Remark 5. *Having $\varepsilon = 0$ in* (19) - (24)*, results in dynamics which is equivalent to the dynamics given in [17]. Thus, the reduced model of the quadrotor with a load suspended through an elastic cable, corresponds to the model of a quadrotor with a load suspended through an inelastic cable.*

The above fact in Remark 5 is later used to show the tracking stability for the system with the load suspended using an elastic cable by using the controller, from [17], which is designed for the system with an inelastic cable. The rest of this section proceeds to define various errors and the associated controllers to track the quadrotor attitude, the load attitude and the load position.

B. Configuration Errors

We now introduce configuration error functions on different manifolds $SO(3)$, S^2 and $\mathbb{R}^3$, see [3]. For the $SO(3)$ manifold, the configuration error function is given as, $\Psi_R = \frac{1}{2}\operatorname{Tr}(I - R_d^T R)^\vee$, while error functions in the Tangent Space $T_R SO(3)$ are defined as:

$$e_R = \frac{1}{2}(R_d^T R - R^T R_d)^\vee, \tag{34}$$

$$e_\Omega = \Omega - R^T R_d \Omega_d, \tag{35}$$

where R_d and Ω_d are desired rotation matrix and angular velocity for the quadrotor. The configuration error Ψ_R can have a maximum value of 2, when the actual rotation matrix is oriented 180° away from the desired rotation matrix R_d and has a value of 0 when $R = R_d$.

Similarly, the configuration error function for the S^2 manifold is given as $\Psi_q = 1 - q_d^T q$, where q_d is the desired load-attitude. Error functions in the tangent Space $T_q S^2$ are given as follows,

$$e_q = \hat{q}^2 q_d, \tag{36}$$

$$e_{\dot{q}} = \dot{q} - (q_d \times \dot{q}_d) \times q. \tag{37}$$

The configuration error Ψ_q will have the values of 0 and 2, when q is aligned parallel and anti-parallel to q_d respectively.

Error functions for position and velocity of the load are given as,

$$e_x = x_L - x_{Ld}, \tag{38}$$

$$e_v = v_L - v_{Ld}, \tag{39}$$

with x_{Ld} and v_{Ld} defined as the desired position and velocity for the load respectively.

Notation: In the above equations, the hat map $\hat{\cdot} : \mathbb{R}^3 \to so(3)$ is defined as $\hat{x}y = x \times y$, $\forall x, y \in \mathbb{R}^3$ & $so(3)$ is the space of skew-symmetric matrices. The vee map, $\vee : so(3) \to \mathbb{R}^3$, is such that $\hat{x}^\vee = x$, $\forall x \in \mathbb{R}^3$.

Having presented the error functions on manifolds, control can be developed to regulate these errors to zero. The following section discusses the control to track the quadrotor attitude, load attitude, and load position about a desired trajectory.

C. Control Design for Quadrotor Attitude, Load Attitude, and Load Position Tracking

Note that the quadrotor attitude dynamics in (12)-(13) is independent of the load attitude and the load position dynamics. Thus, we have the following proposition.

Proposition : 1. [16, Prop. 1] *Almost Global Exponential Stability of Quadrotor Attitude Controlled Flight Mode*

Consider the quadrotor attitude dynamics given by (12)-(13), and consider the moment,

$$M = -\frac{1}{\lambda^2}k_R e_R - \frac{1}{\epsilon}k_\Omega e_\Omega + \Omega \times J_Q\Omega - J_Q(\hat{\Omega}R^T R_d\Omega_d - R^T R_d\dot{\Omega}_d). \quad (40)$$

This can achieve almost global exponential stability for the closed loop tracking error $(e_R, e_\Omega) = (0, 0)$, for positive constants k_R, k_Ω and $0 < \lambda < 1$. Given that the initial conditions satisfy,

$$\Psi_R(R(0), R_d(0)) < 2 \quad (41)$$

$$\|e_\Omega(0)\|^2 < \frac{2}{\lambda_M(J_Q)}\frac{k_R}{\epsilon^2}(2 - \Psi_R(R(0), R_d(0)). \quad (42)$$

where R_d refers to the desired reference trajectory which the controller is tracking. Proof for the above controller is given in [16, Prop. 1].

Next, we present a controller for tracking the load attitude. Note that the load attitude dynamics in (10)-(11) is independent of the load position, and the load attitude is affected only by the perpendicular component of the thrust force $fR\mathbf{e}_3$. Thus we have the following proposition.

Proposition : 2. [16, Prop. 2] *Almost Global Exponential Stability of Load Attitude Controlled Flight Mode*

Consider the load attitude dynamics is given by (10)-(11) along with the quadrotor attitude dynamics (12)-(13), and consider the commanded quadrotor attitude as,

$$R_c := \begin{bmatrix} b_{1c}; & b_{3c} \times b_{1c}; & b_{3c} \end{bmatrix}, \quad \widehat{\Omega}_c = R_c^T\dot{R}_c, \quad (43)$$

where,

$$b_{3c} = \frac{F}{\| F \|}, \quad \text{where,} \quad b_{3c} \in S^2, \quad (44)$$

and,

$$F = F_n - F_{pd} - F_{ff}, \quad (45)$$

$$F_n = -(q_d.q)q, \quad (46)$$

$$F_{pd} = -k_q e_q - k_{\dot{q}} e_{\dot{q}}, \quad (47)$$

$$F_{ff} = m_Q l\langle q, \omega_d\rangle\omega + m_Q l\dot{\omega}_d \times q + 2m_Q\dot{l}(\omega \times q), \quad (48)$$

also,

$$b_{1_c} = -\frac{1}{\|b_{3_c} \times b_{1_d}\|}(b_{3_c} \times (b_{3_c} \times b_{1_d})), \quad (49)$$

where $b_{1_d} \in S^2$ is chosen such that it is not parallel to b_{3_c}. The quadrotor thrust is computed as,

$$f = F.R\mathbf{e}_3, \quad (50)$$

and the Moment is computed using (40) with R_c and Ω_c as desired values.

Initial conditions and the exponential stability of the closed loop tracking error equilibrium $(e_q, e_{\dot{q}}, e_R, e_\Omega) = (0, 0, 0, 0)$ exponential stability follows from [16, Prop. 2].

Remark 6. *Note, that the above control is similar to the control developed in [16, Prop. 2], except for the term* $2m_Q\dot{l}(\omega \times q)$ *which corresponds to the Coriolis effect due to velocity of the load along the direction of the load attitude. Feedforward force given by* (48) *takes* $2m_Q\dot{l}(\omega \times q)$ *into account to develop the feedback control.*

Before presenting the controller required to track the load position, we first show that the system (8) - (11) is equivalent to the system presented in [16], which corresponds to having an inelastic cable when ε tends to zero. Thus, we show that the control technique presented in [16] can also be used to achieve position tracking for load suspended through an elastic cable.

Proposition : 3. *(Main Result) Exponential Stability of Load Position Controlled Flight Mode*

Consider the quadrotor with load suspended through an elastic cable with dynamics given by (8)-(14), and consider the computed load attitude defined as

$$q_c = -\frac{A}{\| A \|} \quad (51)$$

where,

$$A = -k_x e_x - k_v e_v + (m_Q + m_L)(\ddot{x}_L^d + g\mathbf{e}_3) + m_Q l(\dot{q}.\dot{q})q \quad (52)$$

is the desired force to track the load, comprising of feedback force and the feed-forward terms. We assume $\|A\| \neq 0$ and the commanded acceleration is uniformly bounded such that,

$$\|(m_Q + m_L)(\ddot{x}_L^d + g\mathbf{e}_3) + m_Q l(\dot{q}, \dot{q})q\| < B.$$

Furthermore, define F_n as,

$$F_n = (A.q)q. \quad (53)$$

Then, the load position trajectory is within a small neighborhood of a trajectory that exponentially converges to the desired load trajectory.

Stability proof for the load position tracking is shown using the singular perturbation model [9, Theorem 11.2], and requires the conditions expressed in the Lemmas 1-2 to be satisfied.

Lemma 1. *The origin of the reduced model* (33) *for the singular perturbation model* (27)-(28) *is exponentially stable.*

Proof. [16] shows the almost global exponential stability of the reduced model. □

Definition 1. The *Boundary layer system* for the singular perturbation model (27)-(28) is defined as,

$$\frac{\partial y}{\partial \tau} = g(t, x, y + h(t, x), 0), \quad (54)$$

where $y = z - h(t, x)$ with $h(t, x)$ being a well-defined root for the algebraic equation (31) obtained by setting ε to zero, and $t \in [0, t_1]$ is a constant w.r.t. τ. The variable $\tau = (t - t_0)/\varepsilon$ is the stretched time such that, even for a finite time t, $\tau \to \infty$ as $\varepsilon \to 0$.

Lemma 2. *The origin is an exponentially stable equilibrium point of the boundary layer system* (54) *for the singular perturbation model* (27)-(28).

Proof. For the quadrotor with load suspended by spring-damper, the solution for (29) obtained by setting $\varepsilon = 0$ is,

$$\begin{bmatrix} z_1 \\ z_2 \end{bmatrix} = h(t, x) = \begin{bmatrix} \frac{L(\dot{q}.\dot{q}) + F_1}{m_r\bar{k}} \\ 0 \end{bmatrix}. \quad (55)$$

The boundary layer equation for the quadrotor-elastic cable system is given as,

$$\frac{\partial y}{\partial \tau} = g(t, x, y + h(t, x), 0) = \begin{bmatrix} y_2 \\ -m_r\bar{k}(y_1 + \frac{L(\dot{q}.\dot{q}) + F_1}{m_r\bar{k}}) - m_r\bar{c}y_2 + L(\dot{q}.\dot{q}) + F_1 \end{bmatrix}, \quad (56)$$

where, $y_1 = z_1 - \frac{L(\dot{q}.\dot{q})+F_1}{m_r \bar{k}}$ and $y_2 = z_2 - 0$.

The eigenvalues of the linearized system, i.e., the Jacobian matrix $[\partial g/\partial y]$ are given as,

$$\lambda = \frac{-\bar{c}m_r \pm \sqrt{(\bar{c}m_r)^2 - 4\bar{k}m_r}}{2}. \tag{57}$$

Note that $Re(\lambda) < 0$, since $\{\bar{c},\, \bar{k},\, m_r\} > 0$. This proves that the origin of the boundary layer system is exponentially stable. □

Remark 7. *Note that for the boundary layer system to be exponentially stable, we require* $\bar{c} > 0$. *i.e., the damping coefficient in the cable should be non-zero.*

Having satisfied the above conditions, there is a positive constant ε^* such that for all $t_0 \geq 0$, and $0 < \varepsilon < \varepsilon^*$, the singular perturbation system (27), (28) has a unique solution $x(t,\varepsilon)$, $z(t,\varepsilon)$ on $[t_0, \infty)$, and

$$x(t,\varepsilon) - \bar{x}(t) = O(\varepsilon), \tag{58}$$

$$z(t,\varepsilon) - h(t,\bar{x}(t)) - \widehat{y}((t-t_0)/\varepsilon) = O(\varepsilon), \tag{59}$$

hold uniformly for $t \in [t_0, \infty)$, where $\bar{x}(t)$ and $\widehat{y}(t)$ are the solutions of the reduced model (33) and the boundary layer system (54). Also for $t_b > t_0$,

$$z(t,\varepsilon) - h(t,\bar{x}(t)) = O(\varepsilon), \tag{60}$$

uniformly on $[t_b, \infty)$ for $\varepsilon < \varepsilon^{**} \leq \varepsilon^*$, see [9, Theorem 11.2].

Thus, the trajectory of the load position for the complete system (27) - (28) *(quadrotor with load suspended through an elastic cable*) results in being within a small neighborhood of the trajectory of the load position for the reduced model (33) *(quadrotor with load suspended through an inelastic cable)*, thereby establishing the main result in Proposition 3.

IV. Simulation Results

In this section we present a numerical example to validate the controller presented in the previous section. The following equation presents an aggressive reference trajectory for the load and quadrotor yaw angle.

$$x_n(t) = \begin{bmatrix} a_x(1-\cos(2f_1\pi t)) \\ a_y \sin(2f_2\pi t) \\ a_z \cos(2f_3\pi t) \end{bmatrix}, \tag{61}$$

$$\psi(t) \equiv 0 \tag{62}$$

where,

$$a_x = 2,\ a_y = 2.5,\ a_z = 1.5,$$
$$f_1 = \frac{1}{4},\ f_2 = \frac{1}{5},\ f_3 = \frac{1}{7}.$$

The controller from Section III to achieve the position tracking for the system given in (8) - (13) is used. The performance of the controller and the snapshots of the quadrotor at different instants are illustrated in the Figure 2. The respective errors in the quadrotor attitude, load attitude and the load position errors while tracking the desired reference trajectory for the complete system $\varepsilon \neq 0$ and the reduced model $\varepsilon = 0$ are given in the Figure 3. As can be seen from Figure 3 large initial errors of $5\,m$ for the load position converges to zero. The corresponding inputs required to achieve the load position tracking is illustrated

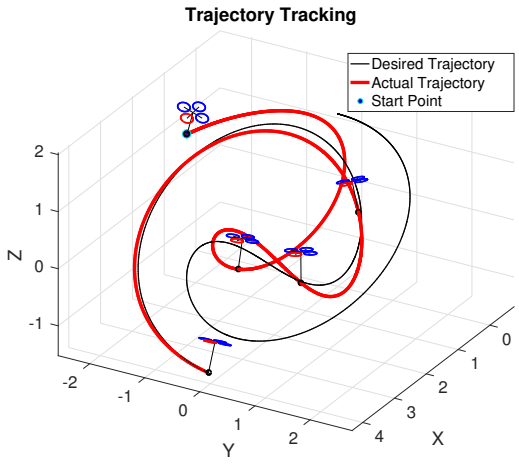

Fig. 2: Load Trajectory Tracking, for load suspended from quadrotor with a cable modeled as spring-damper. Different snapshots of the quadrotor while tracking the reference trajectory is presented here. Red trajectory refers to the actual trajectory where as black represents the desired trajectory. Tracking errors are shown in the Figure 3.

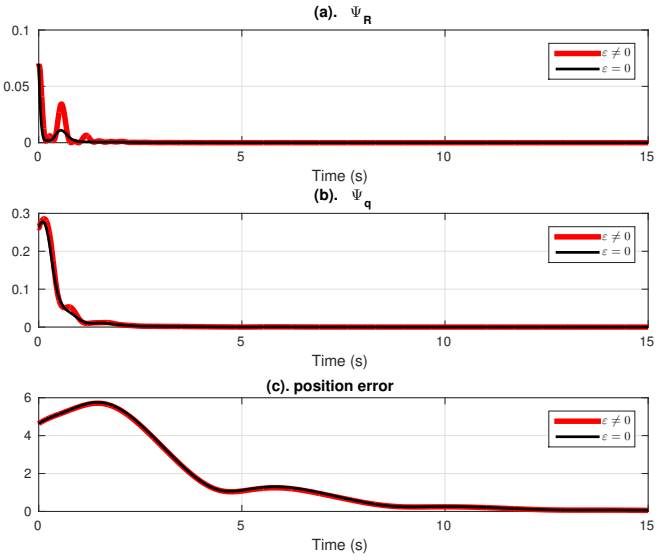

Fig. 3: Tracking errors obtained through simulation while tracking the reference trajectory shown in Figure 2, using the control developed for reduced model. $\varepsilon = 0$ corresponds to the reduced model and $\varepsilon = 0.1 \neq 0$ is the actual system.

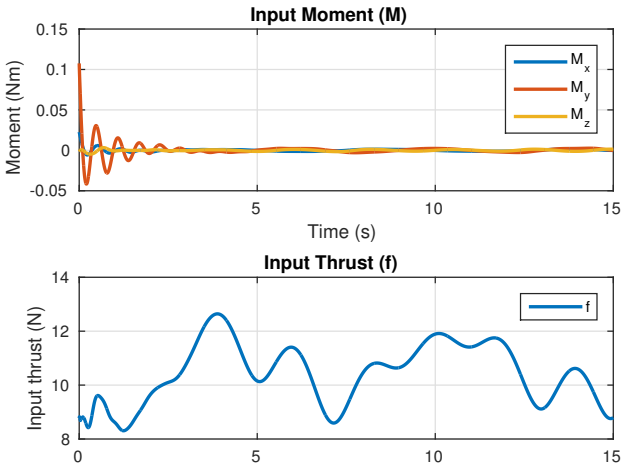

Fig. 4: Inputs for the load tracking for the trajectory given in Figure 2.

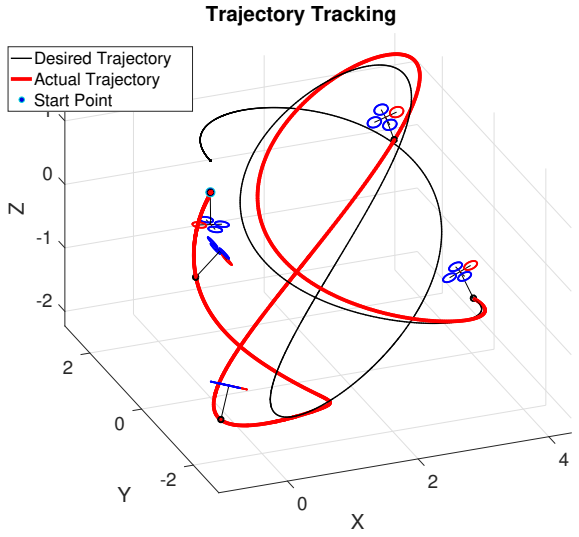

Fig. 5: Trajectory tracking achieved for almost inverted initial condition, where the quadrotor and load are almost inverted and there is a large error in the load position. Tracking errors are shown in Figure 6 for different ε.

in Figure 4. We also present the case with initial condition of quadrotor and load being almost inverted and is illustrated in Figure 5. Thus, showing that the controller works even with large attitude errors. Convergence of the errors for different values of ε corresponding to different spring stiffness and damping is illustrated in the Figure 6.

V. Conclusion

We have addressed the problem of using a quadrotor to transport a point-mass payload suspended through an elastic cable. The coordinate-free dynamics of the entire system is derived where the effects of the cable's elasticity can be seen clearly. We use singular-perturbations to show that the same geometric controller developed for the quadrotor with a load suspended through an inelastic cable works for the case of elastic cable, providing a bounded result. The proposed controller was validated through several numerical results.

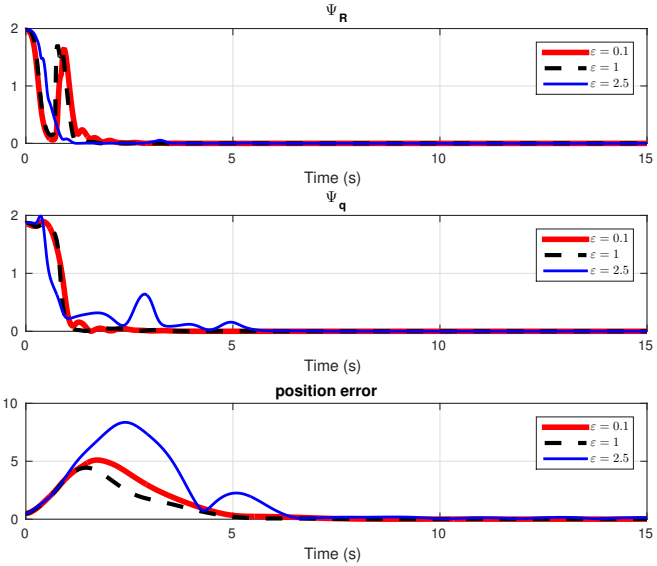

Fig. 6: Errors for different values of $\varepsilon = \{0.1,\ 1,\ 2.5\}$, corresponding to smaller spring stiffness and damping coefficients. As noticed with increase of ε, the errors of the system increase, implying that the actual model cannot be approximated to reduced model for higher ε values.

Appendix

A. Derivation of the Dynamics for the Quadrotor with Load Suspended by Elastic Cable

In this section we present the detailed derivation of the compact equations of motion on manifolds for the quadrotor with the load suspended by an elastic cable, whose dynamics are given by (8) - (14). We derive these dynamics through the Lagrange-d'Alembert's principle of least action. We begin with (7) and expand the terms to obtain,

$$\begin{aligned}\delta \int_{t_0}^{t_1} \Big(&\frac{1}{2} m_Q \langle v_Q, v_Q \rangle + \frac{1}{2} \langle \Omega, J\Omega \rangle + \frac{1}{2} m_L \langle v_L, v_L \rangle \\ &- m_Q g \mathbf{e}_3 . x_Q - m_L g \mathbf{e}_3 . x_L - \frac{1}{2} k (L-l)^2 \Big) dt \\ + \int_{t_0}^{t_1} \Big(&\langle R^T \delta R, \hat{M} \rangle + (\delta x_L - (\delta l) q - l(\delta q)) . f R \mathbf{e}_3 \\ &+ (\delta l) q . (-c \dot{l} q) \Big) dt = 0.\end{aligned} \tag{63}$$

Taking variations on the action integral and substituting

for δx_Q, $\dot{x}_Q$ and $\delta \dot{x}_Q$ from Section II gives,

$$\begin{aligned}
&\int_{t_0}^{t_f} \Big(\delta \dot{x}_L . \big[m_Q (\dot{x}_L - \dot{l} q - l \dot{q}) + m_L \dot{x}_L \big] \\
&\qquad + \delta x_L . \big[- m_Q g \mathbf{e}_3 - m_L g \mathbf{e}_3 + f R \mathbf{e}_3 \big] \Big) dt \\
&+ \int_{t_0}^{t_f} \Big(\delta \dot{l} \big[- m_Q q (\dot{x}_L - \dot{l} q - l \dot{q}) \big] + \delta l \big[- m_Q \dot{q} (\dot{x}_L \\
&\quad - \dot{l} q - l \dot{q}) + m_Q g q \mathbf{e}_3 + k(L-l) - c \dot{l} - q f R \mathbf{e}_3 \big] \Big) dt \\
&\qquad + \int_{t_0}^{t_f} \Big(\delta \dot{q} . \big[- m_Q l (\dot{x}_L - \dot{l} q - l \dot{q}) \big] \\
&+ \delta q . \big[- m_Q \dot{l} (\dot{x}_L - \dot{l} q - l \dot{q}) + m_Q l g \mathbf{e}_3 - l f R \mathbf{e}_3 \big] \Big) dt \\
&\qquad + \int_{t_0}^{t_f} \Big(\dot{\eta} . J \Omega + \eta . \big[J \Omega \times \Omega + M \big] \Big) dt = 0.
\end{aligned} \tag{64}$$

Applying integration by parts and simplifying, we finally have,

$$\begin{aligned}
&\int_{t_0}^{t_f} \Big(\delta x_L . \big[- (m_Q + m_L)(\dot{v}_L + g \mathbf{e}_3) \\
&\qquad + m_Q (\ddot{l} q + 2 \dot{l} \dot{q} + l \ddot{q}) + f R \mathbf{e}_3 \big] \Big) dt \\
&+ \int_{t_0}^{t_f} \Big(\delta l \big[m_Q q . (\dot{v}_L + g \mathbf{e}_3) - m_Q q . (\ddot{l} q + 2 \dot{l} \dot{q} + l \ddot{q}) \\
&\qquad + k(L-l) - c \dot{l} - q . f R \mathbf{e}_3 \big] \Big) dt \\
&\qquad + \int_{t_0}^{t_f} \Big(\xi . \big[q \times m_Q l (\dot{v}_L - \ddot{l} q - 2 \dot{l} \dot{q} - l \ddot{q}) \\
&\qquad + q \times (m_Q l g \mathbf{e}_3 - l f R \mathbf{e}_3) \big] \Big) dt \\
&\qquad + \int_{t_0}^{t_f} \Big(\eta . \big[- J \dot{\Omega} - \Omega \times J \Omega + M \big] \Big) dt = 0.
\end{aligned} \tag{65}$$

For (65) to be valid for all time $t \in [t_0, t_f]$ and for all variations δx_L, δl, ξ and η, the expressions on the right side of the variation has to be equal to zero $\forall\, t$, which results in,

$$(m_Q + m_L)(\dot{v}_L + g \mathbf{e}_3) = m_Q (\ddot{l} q + 2 \dot{l} \dot{q} + l \ddot{q}) + f R \mathbf{e}_3, \tag{66}$$

$$\begin{aligned}
m_Q q . (\dot{v}_L + g \mathbf{e}_3) - m_Q q . (\ddot{l} q + 2 \dot{l} \dot{q} + l \ddot{q}) \\
+ k(L-l) - c \dot{l} - q . f R \mathbf{e}_3 = 0,
\end{aligned} \tag{67}$$

$$\begin{aligned}
q \times [q \times m_Q l (\dot{v}_L - \ddot{l} q - 2 \dot{l} \dot{q} - l \ddot{q}) \\
+ q \times (m_Q l g \mathbf{e}_3 - l f R \mathbf{e}_3)] = 0,
\end{aligned} \tag{68}$$

$$- J \dot{\Omega} - \Omega \times J \Omega + M = 0. \tag{69}$$

Simplifying these equations results in the equations of motion given in (9), (11), (14) and (13).

REFERENCES

[1] V. Agrawal, W. J. Peine, and B. Yao, "Modeling of a closed loop cable-conduit transmission system," in *Robotics and Automation, 2008. ICRA 2008. IEEE International Conference on*, 2008, pp. 3407–3412.

[2] M. Bernard and K. Kondak, "Generic slung load transportation system using small size helicopters," in *Robotics and Automation, 2009. ICRA'09. IEEE International Conference on*, 2009, pp. 3258–3264.

[3] F. Bullo and A. D. Lewis, *Geometric control of mechanical systems: modeling, analysis, and design for simple mechanical control systems*. Springer Science & Business Media, 2004, vol. 49.

[4] M. Cartmell and D. McKenzie, "A review of space tether research," *Progress in Aerospace Sciences*, vol. 44, no. 1, pp. 1–21, 2008.

[5] J. H. Chow, J. J. Allemong, and P. V. Kokotovic, "Singular perturbation analysis of systems with sustained high frequency oscillations," vol. 14, no. 3. Elsevier, 1978, pp. 271–279.

[6] F. A. Goodarzi, D. Lee, and T. Lee, "Geometric control of a quadrotor uav transporting a payload connected via flexible cable," *International Journal of Control, Automation and Systems*, vol. 13, no. 6, pp. 1486–1498, 2015.

[7] F. A. Goodarzi and T. Lee, "Dynamics and control of quadrotor uavs transporting a rigid body connected via flexible cables," in *2015 American Control Conference*, 2015, pp. 4677–4682.

[8] S. Joshi and C. D. Rahn, "Position control of a flexible cable gantry crane: theory and experiment," in *American Control Conference, Proceedings of the 1995*, vol. 4, 1995, pp. 2820–2824.

[9] H. K. Khalil and J. Grizzle, *Nonlinear systems*. Prentice hall New Jersey, 1996, vol. 3.

[10] S. Kim, S. Choi, and H. J. Kim, "Aerial manipulation using a quadrotor with a two dof robotic arm," in *2013 IEEE/RSJ International Conference on Intelligent Robots and Systems*, 2013, pp. 4990–4995.

[11] T. Lee, "Geometric control of multiple quadrotor uavs transporting a cable-suspended rigid body," in *53rd IEEE Conference on Decision and Control*, 2014, pp. 6155–6160.

[12] T. Lee, K. Sreenath, and V. Kumar, "Geometric control of cooperating multiple quadrotor UAVs with a suspended payload," in *IEEE Conference on Decision and Control*, Florence, Italy, Dec. 2013, pp. 5510–5515.

[13] D. Mellinger, M. Shomin, N. Michael, and V. Kumar, "Cooperative grasping and transport using multiple quadrotors," in *Distributed autonomous robotic systems*. Springer, 2013, pp. 545–558.

[14] J. Milnor, *Morse Theory.(AM-51)*. Princeton university press, 2016, vol. 51.

[15] I. Palunko, P. Cruz, and R. Fierro, "Agile load transportation: Safe and efficient load manipulation with aerial robots," *IEEE robotics & automation magazine*, vol. 19, no. 3, pp. 69–79, 2012.

[16] K. Sreenath, T. Lee, and V. Kumar, "Geometric control and differential flatness of a quadrotor UAV with a cable-suspended load," in *IEEE Conference on Decision and Control*, Florence, Italy, Dec. 2013, pp. 2269–2274.

[17] K. Sreenath, N. Michael, and V. Kumar, "Trajectory generation and control of a quadrotor with a cable-suspended load-a differentially-flat hybrid system," in *IEEE International Conference on Robotics and Automation*, 2013, pp. 4888–4895.

[18] S. Tang and V. Kumar, "Mixed integer quadratic program trajectory generation for a quadrotor with a cable-suspended payload," in *2015 IEEE International Conference on Robotics and Automation*, 2015, pp. 2216–2222.

[19] G. Wu and K. Sreenath, "Geometric control of quadrotors transporting a rigid-body load," in *IEEE Conference on Decision and Control*, Los Angeles, CA, Dec. 2014, pp. 6141–6148.